CHARGED PARTICLES, NEUTRALS, AND NEUTRONS

May-Britt Kallenrode
University of Osnabrück, Germany

ABSTRACT

Energetic particles stem from different sources. With a few exceptions acceleration occurs remote from the observer. Energetic particles therefore provide not only tools in the analysis of these acceleration processes but also are probes for plasma conditions between acceleration site and observer. By combining different particles species, in particular charged ones and neutrals, and comparing to electromagnetic radiation, information about particle acceleration, storage, release and propagation can be obtained. In this paper, some aspects of our current understanding of particles are reviewed. The potential of Solar Orbiter to provide information on many of the unsolved problems and to do some important first observations will be addressed.

Key words: solar energetic particles – interplanetary shocks – flares: neutrons – energetic neutrals.

1. INTRODUCTION

One of the prime objectives of Solar Orbiter are in situ measurements in the inner heliosphere in regions not accessed by spacecraft so far. These measurements comprise plasma, fields, and particles from different sources. The particle populations can be characterized as energetic charged particles, which in the innermost heliosphere basically consist of solar energetic particles (SEPs) which should be called solar activity related particles (SARPs) to avoid confusion with the use of the term SEPs in the sense of particles accelerated in a flare. SARPs can be flare accelerated particles (FPAs) and particles accelerated at CME shocks (PACHs). Both populations are related to physically distinct acceleration mechanisms, however, particle events in interplanetary space do not necessarily consist either of FAPs or PACHs. Instead, they can be a mixture of both of them.

PACHs can be observed directly at the shock. Thus simultaneous observations of the accelerating agent and the accelerated particles are possible – although the bulk of the PACHs not necessarily is accelerated locally. FAPs always are accelerated remote from the observer's site, however, additional information on FAPs can be gained from hard electromagnetic radiation and neutrons, which both are secondaries created by the interaction of energetic charged particles with the lower corona or the photosphere, and by mapping the particles back to the solar source regions. On the other hand, particles also can be used as tracers for the large scale coronal and interplanetary magnetic field structures.

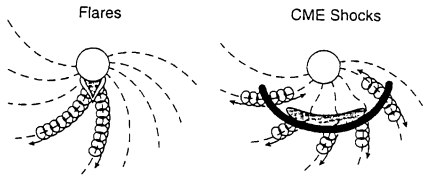

Figure 1. Current paradigm: solar activity related particles (SARPs) can either be accelerated in flares or at shocks (Reames, 1999).

The current classification scheme for SARPs, their acceleration mechanisms and a comparison with secondaries will be given in Chapter 2 with special emphasis on open questions to be addressed by Solar Orbiter. In Chapter 3 neutrals will be briefly discussed, in particular energetic neutral atoms (ENAs).

2. SOLAR ACTIVITY RELATED PARTICLES (SARPS)

Questions on SARPs concern their acceleration and subsequent storage, release and propagation. In this paper I will focus on the aspect of acceleration, the other processes will be mentioned only briefly.

2.1. The Current Paradigm: Two Classes

The current paradigm is based on two classes of flares, impulsive and gradual and leading to two classes of particle events, also termed impulsive and gradual; for a review see Reames (1999).

Proceedings of "Solar Encounter: The First Solar Orbiter Workshop", Puerto de la Cruz, Tenerife, Spain, 14 – 18 May 2001 (ESA SP-493, September 2001)

Table 1. Classes of flares

	impulsive	gradual
Duration SXR	< 1 h	> 1 h
τ SXR	< 10 min	> 10 min
Height	$\leq 10^4$ km	$\sim 5 \cdot 10^4$ km
Volume [cm^3]	$10^{26} - 10^{27}$	$10^{28} - 10^{29}$
energy density	high	low
Hα size	small	large
Duration HXR	< 10 min	> 10 min
Duration μ	< 5 min	> 5 min
Metric Radio	(II),III	II,(III),IV
CME	rare	always

Table 2. Classes of particle events

	^{3}He-rich	gradual
particles	electron rich	proton rich
^{3}He/^{4}He	~ 1	~ 0.0005
Fe/O	~ 1.23	~ 0.15
H/He	~ 10	~ 100
Q_{Fe}	~ 20	~ 14
Duration	hours	days
Long. Distrib.	$< 30°$	$\leq^1 80°$
Metric Radio	III,V	II,III,IV,V
Solar Wind	-	ipl. shock
Event rate	~ 1000/a	~ 10/a

Lets start with the classification of flares. Based on properties of the electromagnetic radiation, in particular its duration or decay constant (Pallavicini et al., 1977; Klein et al., 1983; Ohki et al., 1983; Bai, 1986b; Cane et al., 1986; Daiborg et al., 1987; Cliver et al., 1989), flares can be divided into impulsive and gradual, cf. Table 1. Impulsive flares are small, compact low-lying events with relatively high energy densities. Since in general they are not accompanied by a CME, they also have been termed confined flares (de Jager, 1986). Gradual events, on the other hand, are large events high in the corona with low energy densities. Since they are always accompanied by CMEs, gradual events also have been called eruptive flares. As is evident from the table, classification of flares can be based on different features and is not necessarily unambiguous: a flare might appear gradual in soft X-rays but impulsive in hard X-rays or vice versa. With the observations of CMEs limited to the larger ones, Cane et al. (1986) proposed to use the occurrence of a coronal mass ejection (CME) in gradual events as a clear-cut division. This clear-cut division also is used in Fig. 1.

Let us now turn to the energetic particle events, cf. Tab. 2. SARPs comprise charged flare accelerated particles (FAPs), charged particles accelerated at CME shocks (PACHs), and neutrons produced in the interaction between flare-accelerated solar nuclei and the denser solar atmosphere. An observer in space, however, does not see the acceleration mechanism directly. Instead, ideas about particle acceleration have to be inferred from properties of the particle event, such as time profiles, charge states, and composition, and the parent solar activity, such as flares, disappearing filaments (DFs), and coronal mass ejections (CMEs). Our current paradigm divides flares into two classes, gradual and impulsive, and associates these classes with distinct acceleration and release mechanisms, cf. Fig. 1: in impulsive flares particles are accelerated locally at the flare site and propagate along open field lines connecting to the flare site. Particles thus are FAPs. In gradual events, on the other hand, all acceleration occurs at a CME shock. Thus particles are accelerated over a wide range and escape immediately.

This picture has emerged as follows: the first general classification criterion for particle events was the e/p ratio (Cane et al., 1986) and subsequently the H/He ratio (Kallenrode et al., 1992). In addition, gradual events could be observed at large azimuthal distances while in impulsive events a magnetic connection between observer and a rather small cone around the flare site is required. These observations hinted the importance of a CME driven shock for the acceleration of all or at least additional particles in gradual events, allowing for their wider spread in longitude as well as the high proton abundance.

The analysis of charge states Q_{Fe} of iron gave additional hints and constraints on differences in the acceleration mechanism. Averaged over a large number of impulsive particle events (^{3}He-rich events), Luhn et al. (1987) obtained an average Q_{Fe} of 20.5 ± 1.5 at energies 0.3–2 MeV/nucl compared to the average value of 14 ± 0.2 in gradual events. Similar low charge states in gradual events later also have been observed at higher energies: $Q_{Fe} = 11.0 \pm 0.2$ between 0.5 and 5 MeV/nucl (Mason et al., 1995), $Q_{Fe} = 15.2 \pm 0.7$ between 15 and 70 MeV/nucl (Leske et al., 1995), and $Q_{Fe} = 14.1 \pm 1.4$ between 200 and 600 MeV/nucl (Tylka et al., 1999). High charge states indicate temperatures at the acceleration site of about 10 Mio K in impulsive and 1–2 Mio in gradual flares. Charge states thus are indicative for particle acceleration out of the hot flare material in impulsive events while in gradual events particles are accelerated out of the ambient plasma (corona, solar wind).

This association is supported by peculiarities in composition. Asides from the original division into electron-rich and proton-rich also other particle ratios showed strong variations. The first reported abundance anomaly was concerned with some small events greatly enhanced in the rare isotope ^{3}He (Hsieh & Simpson, 1970). ^{3}He/^{4}He could be of the order of 1, compared to a ratio of $2 \cdot 10^{-4}$ in the solar wind or corona. Large gradual events, on the other hand, show no enrichment above the detection threshold of 0.1. Subsequently, for the ^{3}He-rich events enrichment relative to coronal abundances were also found e.g. in Fe/O (up to 10) and Ne/O (about 4), in Ne/C, Mg/C and Si/C (about

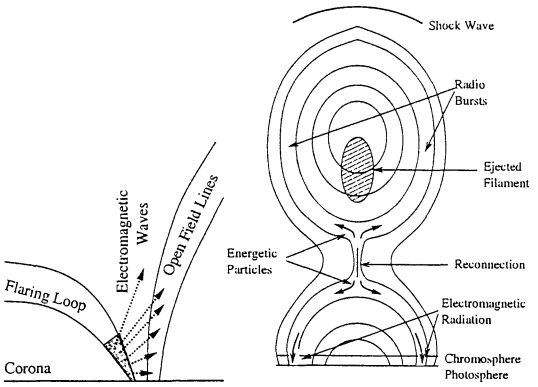

Figure 2. Sketch of particle acceleration due to selective heating in impulsive flares (left) and due to a CME shock in gradual flares (right).

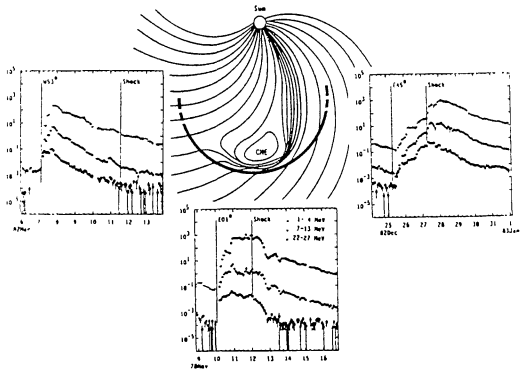

Figure 3. Energetic particle events show different intensity time profiles along the shock front (Reames, 1999).

2.8) and in Fe/C (about 6.7). Other ratios, such as ^{4}He/C, N/C or O/C do not differ significantly from coronal ons; for a review see Reames et al. (1994). The authors also note that heavy element abundances, specifically Fe/C, are not correlated with the ^{3}He/^{4}He ratio. In gradual events, at energies around 1 MeV/nucl abundances approached coronal values with minimal event to event variation (Mazur et al., 1992) while at energies above 10 MeV/nucl an increasing divergence is observed: an enrichment in ^{3}He does not automatically include strong enrichment in other rare species and vice versa.

2.2. Acceleration Mechanisms

These observations can be summarized consistently in a picture of two distinct acceleration processes: in impulsive events acceleration occurs in a flare and particles escape in a rather narrow cone along open field lines, as sketched on the left in Fig. 1, while in gradual events particles are accelerated over a broad range of longitudes at the CME shock. Since particles are picked up out of the ambient medium, they have charge states and abundances resembling the ones in the corona and in the solar wind. Thus the main contributor of particles in gradual events is the shock. In addition, there is reconnection below the CME, cf. right hand side of Fig. 2, accelerating the particle populations that produce electromagnetic radiation over a wide range of frequencies.

2.2.1. Acceleration at a CME-Shock: PACHs

A shock can accelerated particles via three processes which all show distinct features, cf. Scholer & Morfill (1977), for a review see Jones & Ellison (1991). In shock drift acceleration (SDA), also called scatter-free shock acceleration, particles gain energy by drifting in the $\vec{v} \times \vec{B}$-field in the shock front, see e.g. Armstrong (1985). Thus SDA works best for quasi-perpendicular shocks where the electric induction field becomes maximal. In shock drift acceleration particles are scattered back and forth in the plasma streams converging at the shock front, see e.g. Forman & Webb (1985). Diffusive shock acceleration thus is a Fermi 1 process. It dominates in quasi-parallel shocks and, of course, requires sufficient scattering. Stochastic acceleration works in the turbulence behind the shock front, its a Fermi 2 process (Scholer & Morfill, 1977). Depending on the dominant process, particle profiles show distinct features: SDA is characterized by a shock spike around the time of shock passage while diffusive shock acceleration leads to smoother variations and a long lasting high intensity in the event. Stochastic shock acceleration can be seen as a sudden increase in intensity in the turbulent zone behind the shock.

A fundamental problem in all processes is the escape of particles from the acceleration region: once a particle has gained sufficient energy to be significantly faster than the shock, it will escape from the shock front. Then it is lost from the acceleration process and can't be accelerated any further. Energy gain therefore is limited. For particle acceleration up to MeV/nucl or even higher energies relatively strong scattering upstream of the shock is required to feed particles back into the acceleration process. Self-generated waves have been proposed to be responsible for feeding the particles back into the acceleration mechanism, cf. Sect. 2.5.

Since the relative importance of these acceleration mechanisms depends on the angle θ_{Bn} between shock normal and magnetic field, the dominant acceleration mechanism varies along the shock front from shock drift acceleration at the western flank (quasi-perpendicular shock) to diffusive shock acceleration at the eastern flank (quasi-parallel shock). The corresponding characteristics of the acceleration process can be observed directly at the time of shock passage in energies up to some 100 keV (Tsurutani and Lin, 1985; Sanderson et al., 1985) while in MeV energies the dependence on the location of the observer influences the entire particle profile as shown in Fig. 3 (Cane et al., 1988): since at MeV ener-

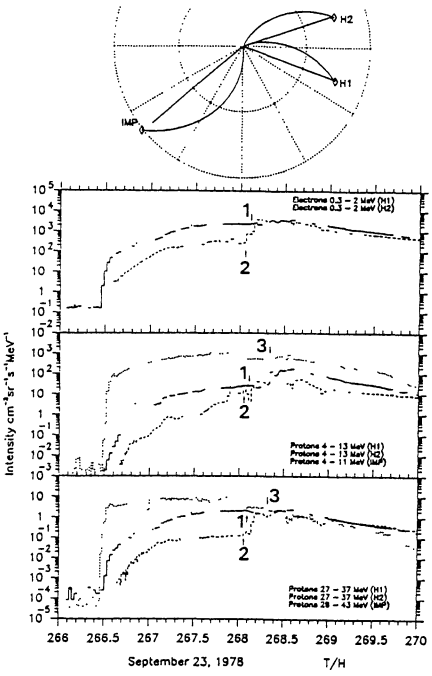

Figure 4. Dependence of particle profiles on location of the observer from multi-spacecraft observations (Helios and IMP).

gies shock acceleration is most efficient close to the nose of the shock, an observer at the shocks eastern flank initially is connected to the efficient nose of the shock and therefore sees a fast rising profile. As the shock propagates outward, its intersection with the observer's magnetic field line moves towards the less efficient flank of the shock and the intensity decays. With a similar reasoning we also can understand the rather flat profiles for observer close to the nose of the shock and the continously rising profiles for observer at the shock's western flank. It should be noted, however, that Fig. 3 is based on a statistical analysis of events observed by one spacecraft only. In multi-spacecraft observations, such as shown in Fig. 4 the variations with location of the observer, although they show the general trend indicated in Fig. 3, can be much smaller.

2.2.2. Acceleration in the Flare: FAPs

The peculiarities in composition in impulsive events require an acceleration mechanism that is highly variable with rigidity and/or Q/A. For ^{3}He-rich flares the process of selective heating has been suggested (Kocharov & Kocharov, 1984; Reames, 1990): particles are accelerated due to reconnection in a compact closed magnetic field loop. Particles then are confined and, on interaction with the denser solar atmosphere, create hard electromagnetic radiation. Electron beams bouncing back and forth along the loop create a wide spectrum of electromagnetic waves which can propagate across the field and, on absorption by the local plasma, accelerate particles. Acceleration occurs for particles with gyrofrequencies comparable to the wave frequency, thus different waves accelerate different particles. Major species, such as H and ^{4}He, absorb most of the wave energy inside the loop while waves in resonance with minor species, such as ^{3}He, are absorbed at larger distances. These latter particles are therefore preferentially accelerated on open field lines and escape into interplanetary space, leading to the peculiarities in composition. Since there is a strong association between ^{3}He-rich events, streaming 10–100 keV electrons (Reames et al., 1985) and type III radio bursts (Reames & Stone, 1986), this process can be compared to the ion conics in the Earth's aurora produced by oblique electromagnetic ion cyclotron (EMIC) waves which in turn are produced by downward streaming electrons (Roth & Temerin, 1997).

If an impulsive flare is violent enough to cause a large scale restructuring of the solar magnetic field, turbulence at long wavelengths will be generated. Large-amplitude long-wavelength Alfvén waves cascade down via shorter waves into the dissipation range where they are absorbed by the thermal plasma. The ions encountered first are those with lowest gyro frequency, namely Fe. The process than continues towards higher Q/A, cascading through resonances with Si, Mg, Ne, later also O and C, eventually He and finally H, leading to the observed enhancements of heavy elements (Miller & Reames, 1996). In addition, Miller & Roberts (1996) found the time scales of such a process to be in agreement with those obtained from the hard electromagnetic radiation.

2.2.3. Questions/Problems

There are some challenges to this picture to ehich Solar Orbiter can contribute valuable observations:

1. Is there a 1:1 correspondence between acceleration processes and flare classes: are particle events either FAPs or PACHs or are there mixed events?
2. in the face of the large number of small and rather slow CMEs observed by SOHO: how does a flare with slow CME (no shock and thus no PACHs) fit into this picture?
3. how do high energetic particles (GeV protons and ions) fit into this picture? Ryan et al. (2000) suggest to use Occam's razor: any model that describes the behavior of lower energy particles in space should extend gracefully to higher energies to explain ground level events (GLEs).

2.3. Interacting and Escaping Particles

This picture of impulsive and gradual flares is sbased on escaping particles observed in interplanetary space. Although we cannot measure them di-

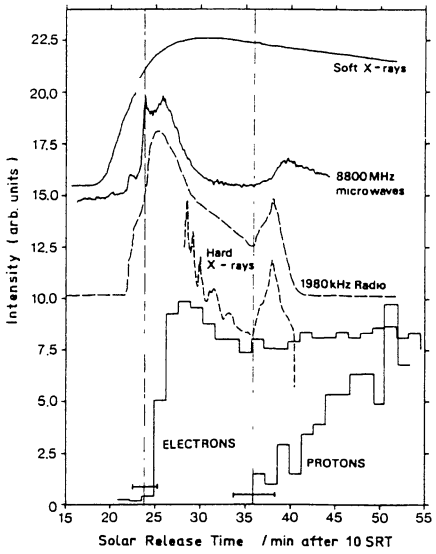

Figure 5. Intensities of interacting and escaping particles, both corrected for travel time (Kallenrode & Wibberenz, 1991).

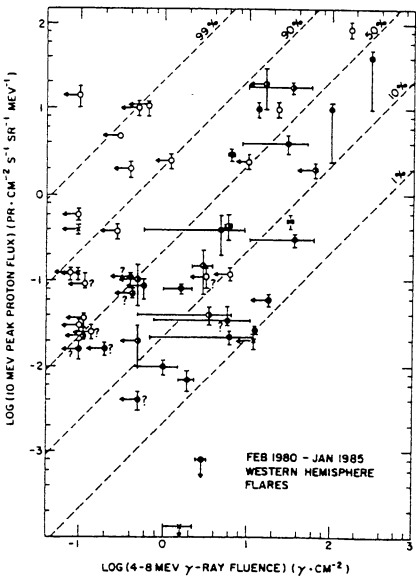

Figure 6. Peak ~10 MeV proton flux vs. 4-8 MeV γ-ray line fluence for well-connected flares. Open circles represent gradual flares, closed ones impulsive (Cliver et al., 1989).

rectly at the flare site, the hard electromagnetic radiation provides information about interacting particles: electrons produce hard X-rays and a γ-ray continuum while nuclei cause γ-ray line emission. The flare' s hard electromagnetic radiation therefore contains information on timing, intensities, spectra, and composition of accelerated particles on the Sun.

2.3.1. Timing

Timing informations can help to relate particle acceleration and release from the Sun to different aspects of solar activity, such as flare acceleration as inferred from interacting particles, radio bursts, or CMEs. Unfortunately, even time scales of the first arriving particles strongly are influenced by interplanetary transport (Kallenrode & Wibberenz, 1990). For an observer at Earth the estimation of onset times therefore is relative inaccurate while the separation of different injections in general becomes impossible. The situation is entirely different within about 0.5 AU (Solar Orbiter will spend roughly half of its time inside 0.5 AU): owing to the close proximity to the Sun, propagation effects have a much smaller influence on particle profiles and thus not only onset times but also multiple particle injections are detectable. Figure 5 shows an example from a perihelion passage of Helios (Kallenrode & Wibberenz, 1991): within the time resolution of the particle instrument injection of energetic electrons occurred simultaneously with radio and microwave emission while the proton injection occurred about ten minutes later simultaneously with a second electron injection with much harder spectrum and a second peak in radio and hard X-ray emission. The authors have interpreted that as evidence for two distinct phases of acceleration, however, due to the incomplete information on solar activity (there were neither CME nor γ-ray observations) and the poor time resolution of the particle event, investigations of similar nature in much better observed events should be extremely valuable.

Compared to Helios, on Solar Orbiter more detailed information on solar activity (CMEs, electromagnetic radiation) will be available. Solar Orbiter will provide a unique opportunity to refine or understanding of phases, modes and steps (Bai, 1986a) of particle acceleration as well as subsequent storage, release, and propagation due to the combination of observations of charged particles, electromagnetic emission, and neutrons. Our understanding would be greatly enhanced, however, if a hard X-ray instrument (preferably an imager) and a γ-ray instrument could be added since both will provide more detailed information about acceleration site and properties of the particles accelerated in the flare.

2.3.2. Intensities and Composition

A comparison of peak intensities of 10 MeV protons observed in interplanetary space in well-connected events with the 4-8 MeV γ-ray line fluence reveals a broad event to event scatter with higher ratios of interacting to escaping particles in impulsive flares (Cliver et al., 1989), cf. Fig. 6.

For interplanetary electrons and γ-ray continua (Kallenrode et al., 1987; Klecker et al., 1990) and for electrons and hard X-rays, cf. Fig. 7, the correlation is similar with a clearer separation between impul-

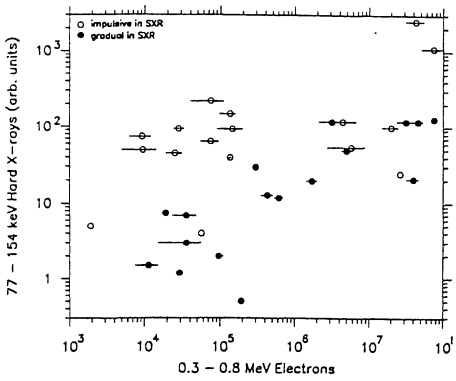

Figure 7. Peak ~0.5 MeV electron flux vs. 77–154 keV hard x-ray flux in gradual (closed) and impulsive (open circles) flares (Kallenrode, 1993)

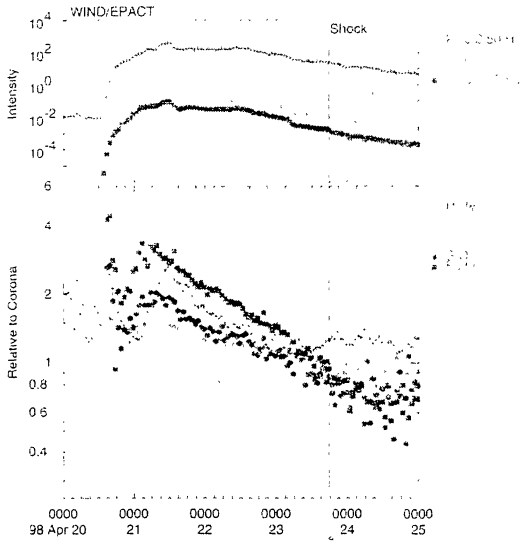

Figure 8. Intensities and variation of composition during a large solar event – composition initially resembles that in impulsive flares and later evolves to that in gradual ones (Tylka et al., 1999)

sive and gradual events and, as in nuclei, a higher ratio of interacting to escaping particles in impulsive flares, suggesting the acceleration of additional protons in gradual flares at the CME shock. For electrons (Klecker et al., 1990; Daiborg et al., 1990) as well as protons (Cliver et al., 1989; Ramaty et al., 1993) the ratio of escaping to interacting particles always is less than 1, indicating particle acceleration in closed loops. Thus the escape of only a few of the flare-accelerated particles is sufficient to create a detectable particle event in interplanetary space. In addition, spectra of escaping particles are harder than that of interacting particles Ramaty et al. (1990, 1993). Combined, these observations point to a highly variable and energy/rigidity dependent escape mechanism. For a better understanding of this escape, the much higher timing information and a comparison with neutrons, both provided by Solar Orbiter, might proof extremely valuable.

Looking at the interacting particles in impulsive and gradual events, one finds: (a) the e/p ratio is the same (Ramaty et al., 1993) while in interplanetary space the e/p is high in impulsive than in gradual flares (Cane et al., 1986; Kallenrode et al., 1992); (b) the spectra are the same (Ramaty et al., 1993) while in interplanetary space spectra are different, in particular in electrons (Moses et al., 1989); (c) the composition is essentially the same (Ramaty et al., 1990, 1993, 1997; Murphy et al., 1991, 1997; Mandzhavidze et al., 1999; Share & Murphy, 1999; Cohen et al., 1999). This points to a common acceleration mechanism for the interacting particles: "in both impulsive and gradual flares the particles that interact and produce γ-rays are always accelerated by the same mechanism that operates in impulsive flares, namely, stochastic acceleration through gyro-resonant wave-particle interactions (Mandzhavidze et al., 1999)i." Then, of course, an important question arises: most likely, in gradual events these particles are trapped in the closed magnetic loops behind the CME. However, as mentioned above, only a small number of particles must escape to create a significant particle event in interplanetary space. And this easily might happen in the dynamic, continuously restructuring magnetic field behind the CME. In that case, we would get a gradual event consisting of both, particles accelerated in the flare and at a CME shock.

2.4. Mixed Events and other Challenges

In fact, observations with ACE suggest that such mixed events are not unusual and can be detected in the analysis of composition and charge states. In some large events, Q_{Fe} shows a distinct peak at low charge states, indicative for particle acceleration out of the ambient medium, with a tail extending up to $Q_{Fe} \approx 20$, indicative for particle acceleration our of the heated flare plasma. In addition, charge states of all heavy ions increase with energy (Oetlicker et al., 1997; Mazur et al., 1999; Möbius et al., 1999). Cohen et al. (1999) inferred from the charge states of twelve elements with energies of 12–60 MeV/nucl source temperatures of $3 - 6 \times 10^6$ K, significantly high than deduced at lower energies.

In addition, abundance variations are not as clear-cut as suggested in the current paradigm. At energies above ~ 100 MeV/nucl Fe/O ratios seem to increase in several of the the largest events observed during the last two solar cycles (Tylka et al., 1997). The example in Fig. 8 shows the evolution of the composition from initial values resembling the ones in impulsive flares to the composition of the ambient medium at the time of shock passage.

This evolution of composition can be interpreted in two different ways. Reames (1999) suggests that everything is done by the shock because (a) flares are two small and (b) a shock working with electron stripping (Reames et al., 1999) and self-generated

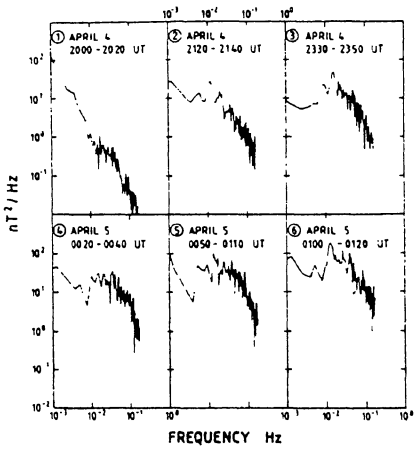

Figure 9. Enhancement of low-frequency waves upstream of the shock due to self-generated turbulence (Sanderson et al., 1985).

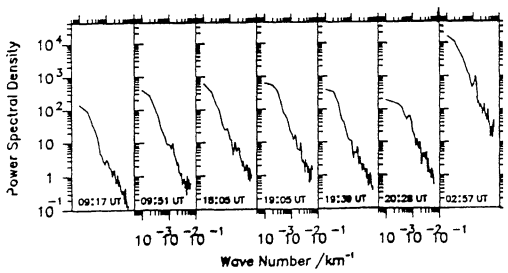

Figure 10. Waves in resonance with 10 MeV protons do not give evidence for enhanced turbulence upstream of the shock. The last frame is taken in the turbulent downstream region and clearly shows an increase in turbulence level.

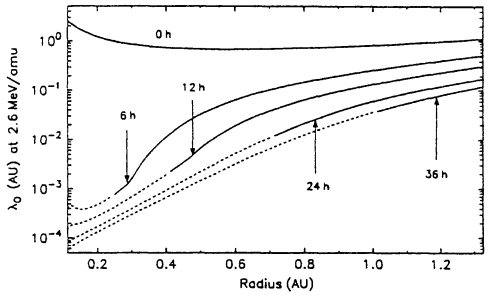

Figure 11. Evolution of the mean free path in a gradual particle event due to self-generated turbulence (Ng et al., 1999). Note that λ is smallest close to the Sun.

waves (Ng et al., 1999) can produce the observed charge states and composition variation. Point (a) rises the questions: why do the charge states at high energies resemble impulsive events – wouldn't it be natural to assume the same acceleration mechanism at work? Although their model tries to answer these questions, it also raises new questions, cf. Cliver (2000): how can two quite different acceleration/transport processes produce identical compositions? And how can the stripping process reproduce charge stated typical for heated plasma? And based on the model of shock-acceleration I would like to add a third question: is there evidence for the proposed mechanism, in particular, where are the waves?

2.5. Shock and Self-Generated Waves

An increase in acceleration efficiency in diffusive shock acceleration due to turbulence generated by streaming protons first has been proposed by Lee (1982) for the bows hock and later for traveling interplanetary shocks (Lee, 1983). For the 12 November 1978 event, Kennel et al. (1986) report good agreement between observations and predictions from the model, cf. Lee (1986) and Völk (1987). While the increase of magnetic field turbulence in low-frequency waves upstream of the shock is clearly visible in Fig. 9, there is no hint for an increase in turbulence at longer wave length in resonance with MeV particles. To my knowledge, observations of self-generated turbulence upstream of a shock in resonance with MeV protons have not been reported sofar. For waves interacting with 10 MeV protons the typical evolution of magnetic field turbulence towards the shock shows no indication for self-generated waves at the observer's site, cf. Fig. 10.

2.6. Where does the Shock Accelerate the Particles?

In the interpretation of the missing upstream turbulence in higher energies we have to be careful: enhanced turbulence should be observed only if the shock is efficient enough to accelerate particle streams of high intensity which, in turn, excite or amplify waves.

In the tens and hundreds of keV/nucl range, efficient particle acceleration occurs even at 1 AU and beyond. In the tens of MeV/nucl range acceleration at the shock preferentially occurs close to the Sun as suggested by Lee & Ryan (1986) from a analytical solution of diffusive shock acceleration (Lee, 1997) or Kahler et al. (1990) from the correlation between CME heights and particle injection (Lockwood et al., 1990; Kahler, 1994; Debrunner et al., 1997). Ng et al. (1999) used a transport model combined with a particle source and self-generated turbulence and inferred that scattering and therefore acceleration, although it evolves with time, is stronger close to the Sun, that is within about 0.3 AU, cf. Fig. 11. Kallenrode (1997) applied a transport model with the shock included as a black-box (Kallenrode & Wibberenz, 1997) to 10eV proton events with interplanetary shock observed by Helios. The evolution of the shock acceleration efficiency S is described by

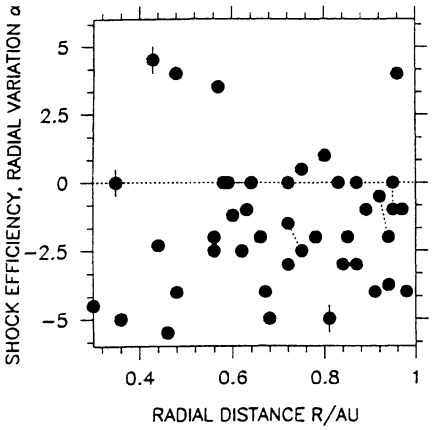

Figure 12. Radial evolution of the particle injection from the shock for 10 MeV protons derived from fits (Kallenrode, 1997). $\alpha = 0$ corresponds to a constant injection, negative αs indicate a decrease in injection as the shock propagates outward.

a power law $S(r) \sim r^{\alpha}$. On average, α equals -2, that is the injection from the shock front decreases like the solar wind density, cf. Fig. 12. Only in a few cases α was positive, indicating strong acceleration at the observer's site.

Solar Orbiter therefore has the unique opportunity to *catch the shock red-handed* while it accelerates MeV particles. In addition, Solar Orbiter will provide insights into the details of the acceleration mechanism, the relative importance of self-generated turbulence at high energies, and the dependence of acceleration efficiency on shock parameters, in particular the local geometry θ_{Bn}.

2.7. Storage and Release

Let us now turn back from the shock to the flare. While particles accelerated at the shock can freely escape (ones they have managed to overcome the turbulent upstream regions), particles accelerated in the flare, according to the scenario presented above, should be confined in a closed loop. Thus storage and release are required because (1) only a small fraction of the accelerated particles is also observed in interplanetary space (Cliver et al., 1989; Daiborg et al., 1990; Klecker et al., 1990; Ramaty et al., 1993) and (2) the spectra of escaping particles are harder than that of interacting particles (Ramaty et al., 1990, 1993), implying an energy-dependent escape process. Thus some mechanisms for particle storage and escape seem to be requires. One might speculate about cross-field diffusion and selective heating being responsible for particle escape in confined flares while the rearrangement of magnetic field lines during a CME might allow particle escape in eruptive flares. This holds even in cases where the CME is too slow to drive a shock (about 2/3 of the CMEs are too slow to drive a shock (Burkepile & St. Cyr, 1993; St. Cyr et al., 2000)): here rearrangement of field liens might support particle escape, probably even over a wider range than in the ^{3}He rich events. These particle events are likely to correspond to the impulsive electron-rich events in Cane et al. (1986) and Kallenrode et al. (1992). Again, Solar Orbiter will provide valuable information from the neutrals and from timing.

2.8. Long-duration γ-ray Events

In long-duration γ-ray flares (LDGRFs) (Ryan et al., 2000) γ-ray line emission at energies above 50 MeV can last for many hours (Kanbach et al., 1993), implying either a prolonged acceleration or efficient storage. Storage is unlikely since such high energetic particles certainly would be lost into the denser solar atmosphere in time. LDGRFs also cannot be understood in terms of backward propagating nuclei accelerated at the outward propagating CME because the thick-target hard X-ray emission resulting from this process is not observed (Murphy et al., 1999; Ramaty et al., 1997). Alternatively, particles could have been accelerated in large static loops filled with MHD turbulence (Ryan & Lee, 1991) or in the electrostatic potential behind the CME in the reconnection sheet (Litvinenko & Somov, 1995).

These long-duration γ-ray flares are different from the longer-lasting hard X-ray events because these in general show evidence for fragmented energy release (van den Oord, 1993): the long-lasting hard electromagnetic emission does not show a rather smooth profile but consists of a large number of elementary bursts which are similar to impulsive events. Thus in that long-duration hard X-ray events, particle acceleration seems to occur repeatedly in the same way as in impulsive events.

2.9. Propagation

One of the long-standing problems in the analysis of interplanetary transport is the discrepancy problem between particle mean free paths (mfps) derived from fits of a transport equation on observed particle profiles and mfps derived from the analysis of magnetic field fluctuation, cf. Fig. 13 (Hasselmann & Wibberenz, 1970; Wanner & Wibberenz, 1993). This has led to a reinterpretation of magnetic field turbulence in terms of two-dimensional dynamical turbulence (Matthaeus et al., 1990; Bieber et al., 1994). Alternatively, radially propagating Alfvén waves have been suggested (Jaekel et al., 1994). The latter idea has been tempting in so far as the discrepancy appears to increase with radial distance of the observer from the Sun.

Solar Orbiter will help to gain a better understanding of interplanetary propagation because due to its close approach to the Sun
(a) fits on particle events will be more accurate since

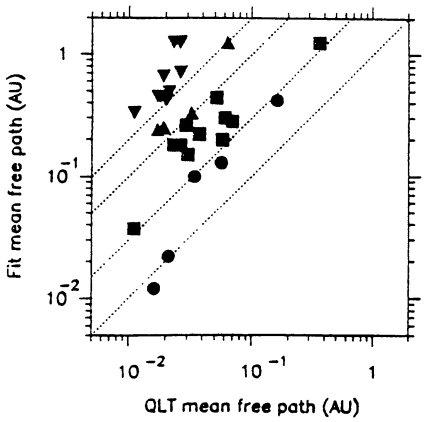

Figure 13. Scattering mean free paths derived from fits vs. those from the analysis of magnetic field fluctuations (Wanner, 1993).

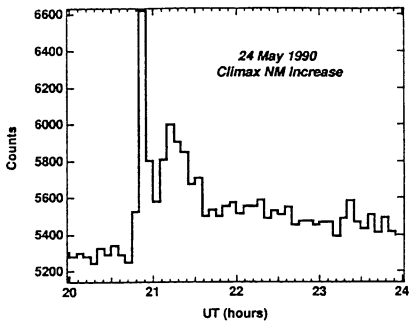

Figure 14. Climax neutron monitor count rates (5-min averages) for the 24 May 1990 GLE (Debrunner et al., 1997).

the field line is more radial and owing to the smaller distances the time scales of the event are smaller and thus the solar wind effects on propagation, in particular adiabatic deceleration, are less pronounced; and (b) certain interpretations of magnetic field fluctuations can be confirmed or discarded.

2.10. Neutrons

The existence of energetic (secondary) neutrons due to the interaction of energetic solar flare protons was first proposed by Biermann et al. (1951). They were first detected with the γ-ray spectrometer on SMM following the 21 June 1980 flare (Chupp et al., 1982) and later, following the 3 June 1982 event simultaneously in space and with neutron monitors on Earth (Chupp et al., 1987; Debrunner et al., 1983).

The largest solar neutron increase reported so far, is the 24 May 1990 event (Debrunner et al., 1997), cf. Figure 14: starting at the time of the flare, a neutron increase lasting for about 25 min (some of which is obscured by the second increase) was observed by

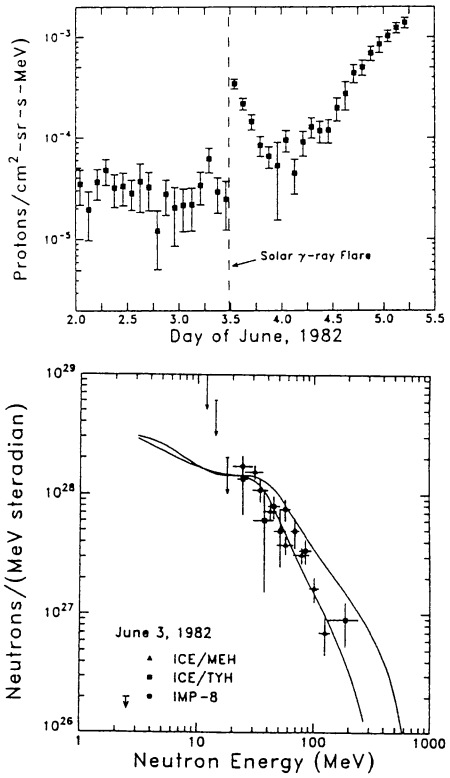

Figure 15. Identification of protons from neutron decay prior to the onset of the real proton event in 25–45 MeV protons (top), and reconstructed emitted neutron spectrum (bottom) (Evenson et al., 1990).

neutron monitors on Earth's dayside. The solar protons started as a second increase about 13 min later on both day- and nightside. It lasted 8 hours and was highly isotropic for more than an hour. In addition, γ-rays with energies up to 100 MeV have been observed (Talon et al., 1993). A similarly energetic event was the 6 November 97 flare during which neutrons were detected, too (Matsabura et al., 1999).

Since the maximum distance a neutron can reach is determined by its speed and its average life time, only neutrons with energies above 100 MeV can be observed at Earth orbit. Low-energy neutrons so far have be measured only indirectly by way of the proton weak decay product as an early sharp increase on proton intensity starting simultaneously with the flare's γ-ray emission (Evenson et al., 1983), cf. Figure 15. Converting the proton intensities to estimated neutron fluxes at the Sun and combining with the direct observations, a composite spectrum spanning three orders of magnitude in energy can be constructed (Chupp et al., 1987; Evenson et al., 1990).

Here the advantage of Solar Orbiter is obvious: its low orbit for the first time will allow the direct measurement of low energy neutrons produced in a flare (with the threshold in neutron energy depending on the position of Solar Orbiter). These observations

will greatly improve our understanding of particle acceleration and release processes.

3. NEUTRALS

Neutral atoms with energies from eV to more than 100 keV are widespread in the heliosphere. They can be divided into two populations: the low energetic neutrals of the local interstellar medium (LISM) and the energetic neutrals in the neutral solar wind or in the energetic neutral atoms (ENAs).

Neutrals do not interact with the ambient plasma and field. Thus their direction of flight is preserved and they can be used as tools to map remote objects such as magnetospheres or the heliosphere. In addition, since there is insignificant energy transfer in the charge exchange, the energy of the ion prior to the interaction is preserved.

3.1. Neutral Solar Wind

The existence of neutral hydrogen in the corona is visible as Lα corona up to distances of about 3 solar radii. These neutrals are closely coupled to the solar wind with relative densities between 10^{-6} and 10^{-7}. Their impact on the solar wind plasma therefore is negligible. The solar wind is a trace population originating from the solar wind plasma by charge exchange. Solar Orbiter will be able to provide the first in-situ measurements of the neutral solar wind, which at Earth's orbit would require a much larger detector. The detailed measurement and understanding of the neutral solar wind will help to refine the physical models of the Lα corona, complement the remote sensing observations of the corona and thus will enhance our understanding of the coronal plasma processes and wave-particle interactions within a few solar radii around the Sun.

Since coronal mass ejections (CMEs) include a wide range of ions with charge distributions originating from very cold to very hot coronal plasma, one would also expect to find neutrals in the CME-related solar wind. Again, owing to its low orbit, Solar Orbiter is in a good position to detect and analyze this trace population. Neutrals in CMEs are not influenced by the magnetic field and thus they might even provide information about the trigger process in a CME.

3.2. Energetic Neutral Atoms (ENAs)

Neutral particles cannot be accelerated easily under solar system conditions. Energetic neutral atoms (ENAs) therefore are generated by charge exchange between energetic charged particles and neutral hydrogen which is abundant in the heliosphere, as first suggested by Dessler & Parker (1959).

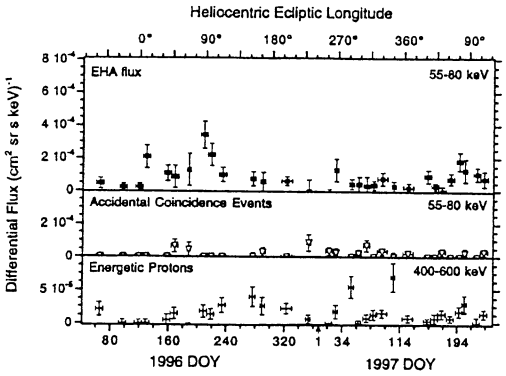

FIG. 6a

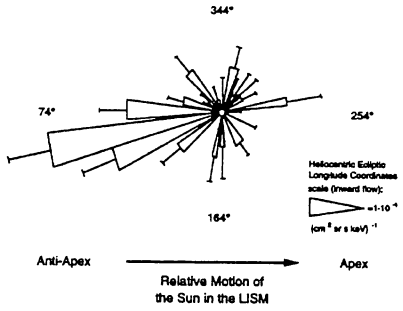

FIG. 6b

Figure 16. Distribution of energetic hydrogen atoms (EHAs) in the heliosphere as measured with HSTOF on Soho in the time period 1996 Doy 203 to 1997 Doy 200. The peak of the distribution is in the general direction of the heliotail or the antiapex (Hilchenbach et al., 1998).

The cross section for charge exchange strongly decreases with energy (Kimura et al., 1993; Kingdon & Ferland, 1996), thus ENAs can be expected up to energies of about 100 KeV only. In addition, ENA energy spectra generally decrease even more rapidly with increasing energy than the original ion spectra. The parent charged particle population basically are protons because multiply ionized particles would require multiple charge-exchange processes to become neutral; exceptions are regions with high densities of neutrals, such as the neutral coma of comets (Cravens, 1997), or planetary atmospheres, such as Venus (Grünwaldt et al., 1997).

The neutral hydrogen is from the LISM, the neutral solar wind, or neutrals produced by neutralization on interplanetary dust particles close to the sun. The charged particles can be the solar wind, SARPs, or anomalous cosmic rays (ACRs); galactic cosmic rays (GCRs) are not a likely source population since their energies are too high. ENAs can be used as tools to probe remote parts of the magnetosphere and heliosphere (Hsieh et al., 1980, 1992), in particular the source regions of the parent energetic particle population. Magnetospheric ENAs were first detected by Roelof (1987), heliospheric ones with HSTOF on SOHO (Hovestadt et al., 1995).

Figure 16 summarizes the observations of heliospheric ENAs, in this case energetic hydrogen atoms (EHAs), in the energy range 55–80 keV for quiet times (when interplanetary charged particle flux was low) as a time series with the view direction of HSTOF indicated in its upper panel. The middle panel gives background rates, the lower one energetic protons. The ENA flux correlates neither with background nor solar protons. In the lower panel the time series is translated into the angular distribution of ENAs in the ecliptic plane with the motion of the Sun relative to the local interstellar medium indicated according to the measurements of Ulysses (Geiss & Witte, 1996). The peak of the distribution is in the general direction of the heliotail or the anti-apex. This is in agreement with the proposed apex-antiapex asymmetry of ACRs (Czechowski et al., 1995).

4. SUMMARY

Of all the interesting and new things Solar Orbiter can do, here just the most important ones are summarized. Some 'Firsts' of the Solar Orbiter Mission include:

- direct observation of low energetic neutrons.
- measurement of the neutral solar wind.
- detection of neutrals in CME-related solar wind.
- energetic particles from microflares?
- Catch the shock redhanded?

In addition, Solar Orbiter will help refine our understanding in many aspects. In particular, it will

- determine the source conditions for different particle species from their composition, charge states, energy spectra, angular distributions, and temporal evolution.
- study MeV particle acceleration at the shock, in particular the importance of self-generated turbulence and the variation of acceleration efficiency with θ_{Bn}.
- probe magnetic field structures with energetic particles to understand storage, release and propagation.

REFERENCES

Armstrong, T.P., M.E. Pesses, and R.B. Decker, 1985, in Geophys. Mon. 35, AGU

Bai, T., 1986, ApJ 308, 912

Bai, T., 1986, ApJ 311, 437

Bieber, J.W., et al., 1994, ApJ 420, 294

Biermann, L., O. Haxel, and A. Schlüter, 1951, Z. Naturf. 62, 47

Burkepile, J.T., & O.C. St. Cyr, 1993, NCAR/TN-369+STR

Cane, H.V., R.E. McGuire, and T.T. von Rosenvinge, 1986, ApJ 301, 448

Cane, H.V., D.V. Reames, and T.T. von Rosenvinge, 1988, JGR 93, 9555

Chupp, E.L. and others, 1982, ApJ 263, L95

Chupp, E.L., et al., 1987, ApJ 318, 913

Cliver, E.W., 2000, in Acceleration and transport of energetic particles observed in the heliosphere: ACE 2000 Symp. (eds. R.A. Mewaldt et al), AIP CP528, 21

Cliver, E.W., et al., 1989, ApJ 343, 953

Cohen, C.M.S., et al., 1999, GRL 26, 149

Cravens, T.E., 1997, GRL 24, 105

Czechowsky, A., S. Grzedzielski, and I. Mostafa, 1995, A&A 297, 892

Daiborg, E.I., et al., 1987, Proc. 20th ICRC 3, 45

Daiborg, E.I., et al., 1990, Proc. 21st ICRC 5, 96

Debrunner, H., et al., 1983, Proc. 18th ICRC 4, 75

Debrunner, H., et al., 1997, ApJ 479, 997

de Jager, C., 1986, Space Sci. Rec. 40, 43

Dessler, A.J., and E.N. Parker, 1959, JGR 64, 2239

Evenson, P., P. Meyer, and K.R. Pyle, 1983, ApJ 274, 875

Evenson, P., P. Kroeger, P. Meyer, and D.V. Reames, 1990, ApJ Suppl. 73, 273

Forman, M.A., and G.M. Webb, 1985, Geophys. Mon. 34, AGU,

Geiss, J., and M. Witte, 1996, Space Sci. Rev. 78, 229

Grünwaldt, H., et al., 1997, GRL 24, 1163

Hasselmann, K., and G. Wibberenz, 1970, ApJ 162, 1049

Hilchenbach, M., et al., 1990, ApJ 503, 916

Hovestadt, D., et al., 1995, Solar Phys. 162, 441

Hsieh, K.C., and J.A. Simpson, 1970, ApJ 162, L191

Hsieh, K.C. et al., 1980, HELENA proposal, NASA

Hsieh, K.C., K.L. Shih, J.R. Jokipii, and A. Grzedzielski, 1992, ApJ 393, 756

Jaekel, U., W. Wanner, R. Schlickeiser, and G. Wibberenz, 1994, A&A

Jones, F.C., and D.C. Ellison, 1991, Space Sci. Rev. 58, 259

Kahler, S.W., D.V. Reames, and N.R. Sheeley, Jr., 1990, Proc. 21st ICRC 5, 183

Kahler, S.W., ApJ 428, 837

Kallenrode, M.-B., 1993, Habil. thesis, Univ. Kiel

Kallenrode, M.-B., 1997, JGR 102, 22 335

Kallenrode, M.-B., and G. Wibberenz, 1990, Proc. 21st ICRC 5, 229

Kallenrode, M.-B., and G. Wibberenz, 1991, ApJ 376, 787

Kallenrode, M.-B., and G. Wibberenz, 1997, JGR 102, 22 311

Kallenrode, M.-B., E. Rieger, G. Wibberenz, and D.J. Forrest, 1987, Proc. 20th ICRC 3, 70

Kallenrode, M.-B., E.W. Cliver, and G. Wibberenz, 1992, ApJ 391, 370

Kanbach, G., et al., 1993, A&A Suppl. 97, 349

Kennel, E.F., et al., 1986, JGR 91, 11917

Kimura, M., N.F. Lane, and A. Dalgarno, 1993, ApJ 405, 801

Kingdon, J.B., and G.J. Ferland, 1996, ApJ Suppl., 106, 205

Klein, L., et al., 1983, Solar Phys. 84, 195

Klecker, B., et al., 1990, Proc. 21st ICRC 5, 80

Kocharov, L.G., and G.E. Kocharov, 1984, Space Sci. Rev., 38, 89

Lee, M.A., 1982, JGR 87, 5063

Lee, M.A., 1983, JGR 88, 6109

Lee, M.A., 1986, in The Sun and the heliosphere in three dimensions (ed. R.G. Marsden), Reidel, 305

Lee, M.A., 1997, in *Coronal mass ejections* AGU, p. 227

Lee, M.A., and J.M. Ryan, 1986, ApJ 303, 829

Leske, R.A., et al., 1995, ApJ 452, L149

Litvinenko, Y., and B. Somov, 1995, Solar Phys. 158, 317

Lockwood, J.A., H. Debrunner, E.O. Flückiger, and H. Graedel, 1990, ApJ 355, 287

Luhn, A., B. Klecker, D. Hovestadt, and E. Möbius, 1987, ApJ 317, 951

Mandzhavidze, N., and R. Ramaty, and B. Kozlovsky, 1999, ApJ 518, 918

Mason, G.M., J.E. Mazur, M.D. Looper, and R.A. Mewaldt, 1995, ApJ 452, 901

Matsabura, Y., et al., 1999, Proc. 26th ICRC, 6, 46

Matthaeus, W.H., M.L. Goldstein, and D.A. Roberts, 1990, JGR 95, 20 673

Mazur, J.E., G.M. Mason, B. Klecker, and R.E. McGuire, 1992, ApJ 401, 398

Mazur, J.E., 1999, et al., GRL 26, 173

Miller, J.A., and D.V. Reames, 1996, in High energy solar physics (eds. R. Ramaty, N. Mandzhavidze, X.-M. Hua), AIP Conf. Proc. 374, 450

Miller, J.A., and D.A. Roberts, 1996, ApJ 452, 912

Möbius, E., et al., 1999, GRL 26, 145

Moses, D., W.D. Dröge, P. Meyer, and P. Evenson, 1989, ApJ 346, 523

Murphy, R.J., R. Ramaty, B. Kozlovsky, and D.V. Reames, 1991, ApJ 371, 793

Murphy, R.J., et al., 1997, ApJ 490, 883

Murphy, R.J., G.H. Share, K.W. Delsignore, and X.-M. Hua, 1999, ApJ 510, 1011

Ng, C.K., D.V. Reames, and A.J. Tylka, 1999, GRL 26, 2145

Oetlicker, M., et al., 1997, ApJ 477, 495

Ohki, K., T. Takakura, B. Tsumata, and N. Nitta, 1983, Solar Phys. 86, 301

Pallavicini, R., S. Serio, and G.S. Vaiana, 1977, ApJ 216, 108

Ramaty, R., R.J. Murphy, and J.A. Miller, 1990, in Particle Astrophysics (eds. W.V. Jones, F.J. Kerr, and J.F. Ormes), AIP, 143

Ramaty, R., et al., 1993, Adv. Space Res. 13(9), 275

Ramaty, R., N. Mandzhavidze, C. Barat, and G. Trottet, 1997, ApJ 479, 458

Reames, D.V., 1990, ApJ Suppl. 73, 253

Reames, D.V., 1999, Space Sci. Rev. 90, 413

Reames, D.V., and R.G. Stone, 1985, ApJ 308, 902

Reames, D.V., T.T. von Rosenvinge, and R.P. Lin, 1985, ApJ 292, 716

Reames, D.V., J.P. Meyer, and T.T. von Rosenvinge, 1994, ApJ Suppl. 90, 649

Reames, D.V., C.K. Ng, and A.J. Tylka, 1999, GRL 26, 3585

Roelof, E.C., 1987, GRL 14, 652

Roth, I., and M. Temerin, 1997, ApJ 477, 940

Ryan, J.M., Space Sci. Rev., in press

Ryan, J.M., and M.A. Lee, 1991, ApJ 368, 316

Ryan, J.M., J.A. Lockwood, and H. Debrunner, 2000, Space Sci. Rev. 93, 35

Sanderson, T.R., et al., 1985, JGR 90, 3974

Scholer, M., and G. Morfill, 1977, PHG-AFB Spec. Rep. 209, 221

Share, G.H., and R.J. Murphy, 1999, Proc. 26th ICRC 6, 13

St. Cyr, et al., JGR 105, 2000, 18 169

Talon, R., et al., 1993, Solar Phys. 147, 137

Tsurutani, B.T., and R.P. Lin, 1985, JGR 90, 1

Tylka, A.J., et al., 1995, ApJ 444, L109

Tylka, A.J., W.F. Dietrich, and R. Boberg, 1997, Proc. 25th ICRC 1, 101

Tylka, A.J., and D.V. Reames, and C.K. Ng, 1999, GRL 26, 2141

van den Oord, G.H.J. (ed.), 1993, Fragmented energy release in Sun and Stars, Kluwer

Völk, H.J., 1987, Proc. 20th ICRC 7, 157

Wanner, W., 1993, PhD Thesis, Univ. Kiel

Wanner, W., and G. Wibberenz, JGR 98, 3513